HOKKAIDO UNIVERSITY

Title	Mechanical evaluation of hip pads to protect against fracture of elderly femurs in falls
Author(s)	Tadano, Shigeru; Nakatsuchi, Hiroki; Goto, Naoko et al.
Citation	Bio-Medical Materials and Engineering, 21(4), 235-246 https://doi.org/10.3233/BME-2011-0672
Issue Date	2011
Doc URL	https://hdl.handle.net/2115/48773
Type	journal article
File Information	BMME21-4_235-246.pdf

Hokkaido University Collection of Scholarly and Academic Papers : HUSCAP

Mechanical Evaluation of Hip-Pads to Protect Against Fracture of Elderly Femurs in Falls

Shigeru TADANO[1], Hiroki NAKATSUCHI[2], Naoko GOTO[3],

Kazuhiro FUJISAKI[4], Yukio NAKATSUCHI[5]

[1] Division of Human Mechanical Systems and Design, Graduate School of Engineering, Hokkaido University, 060-8628 Japan

[2] Postdoctoral fellow, Division of Human Mechanical Systems and Design

[3] Formerly Master Course Student, presently TOSHIBA Corporation, 567-0013 Japan

[4] Formerly Doctor Course Student, presently Division of Human Mechanical Systems and Design

[5] Orthopedic Surgery, Marunouchi Hospital, 390-8601 Japan

Corresponding author:

Shigeru TADANO, Dr. Eng.

Professor, Division of Human Mechanical Systems and Design, Graduate School of Engineering, Hokkaido University, N13 W8, Kita-ku Sapporo, 060-8628 Japan,

TEL & FAX: +81-11-706-6405, Email: tadano@eng.hokudai.ac.jp

Word count: 3,443 words (Introduction through Conclusions)

Abstract

Hip fracture in the aged easily occurs by falls and may cause these persons to become bedridden. Hip pads are effective in protecting hip fracture as they directly deflect and absorb the impact forces by falls. It is necessary for the material and the structure of hip pads to be designed to realize both high impact absorption and compliance (comfort during wearing). In this report, an impact testing system was developed to test the impact absorbing performance of hip pad with air cushions designed by the research group. The impact absorbing performance was evaluated by the impact load, collision time, and maximum load. To confirm the effectiveness in protecting against hip fracture, an impact force was applied to the greater trochanter of the human femur and the degree of fracture was measured by X-ray examination. As a result, the hip pad with air cushions had a high impact absorbing performance and was sufficiently effective to protect against hip fracture.

Keywords:

Biomechanics, Hip pad, Hip fracture, Fall, Impact test

1. Introduction

The femoral neck and trochanteric region are easily fractured by falls in aged persons because of the lowering in bone mineral density and physical depression accompanying aging [(1)]. When ambulatory ability is impaired by hip fracture, the risk of becoming bedridden is high, and it is an urgent problem to prevent hip fractures in aged persons by falls. Hip fracture prevention methods include exercises like muscle training [(2),(3)], drug treatment [(4)] to prevent the reduction in bone mineral density, and the application of hip pads to absorb impact forces directly [(5)-(18)]. Hip pads are especially effective in protecting hip fracture in patients with osteoporosis over 80 years old because they directly deflect and absorb impact forces. However, hip pads need to be worn 24 hours a day. It is necessary to ensure the compliance that is one of the important factors to feel comfort during the wearing of hip pads.

Commercial hip pads can be divided into two types based on the materials and structure. One is soft hip pads made of soft materials like gel and elastomer and the other is hard hip pads with a shell-shape made of harder materials like plastics. Soft hip pads provide a higher degree of comfort during wearing but they are heavy and bulky. While, hard hip pads provide higher impact force absorption but they are less comfort during wearing due to the use of harder materials. Both hip pads are uncomfortable in bed where hip fractures by falls occur frequently. To prevent hip fracture by falls, hip pads should provide both performances of a higher degree

of comfort and impact force absorption effectively during long duration of wearing, even in bed.

Our research group has designed a new hip pad with air cushions to be satisfied with both performances. The hip pad is expected to have high force attenuation effectiveness because it absorbs impact forces by both air and the sponge properties of the cells. In addition, when a person lies on the hip pad, it becomes thinner by deflation of the cells. This results in a decrease in discomfort during wearing even in bed. In this work, the impact absorbing performances were compared between this hip pad with air cushions and commercial hip pads by using a dropped-weight impact testing system. Further, to confirm the effectiveness in protection against hip fracture, an impact force was applied to the greater trochanter of the human femur and the degree of fracture was measured by X-ray examinations.

2. Impact absorbing performance of hip pads

2.1 The hip pad with air cushions

Two kinds of hip pads are available commercially. One absorbs impact forces using soft materials like gel, rubber or soft plastics. The other kind is shell-shaped and deflects the impact forces using hard materials. Both kinds of hip pads are sewed into or placed in pockets of the right and left greater trochanter areas of special underpants. Soft hip pads are superior in comfort during wearing due to the use of soft materials, but they are inferior in force attenuation

effectiveness. In contrast, hard hip pads are superior in force attenuation effectiveness, but are inferior in comfort because of the harder materials. Discomfort during wearing causes a decrease in wearing rates for hip pads. Hence, to protect against hip fracture, hip pads need to provide both high degree of comfort during wearing and high force attenuation effectiveness.

The research group has been developing a hip pad with high degree of comfort during wearing and force attenuation effectiveness. Figure 1 shows a prototype of this hip pad with air cushions, it consists of thirteen hexagonal cells and weighting 0.53 N (54.5g). The hip pad can fit the entire curved surface of the greater trochanter due to the 2 mm intervals between neighboring cells. Each cell consists of a hexagonal shaped column of sponge and a film covering the sponge and air enclosed in the cell. A 0.4 mm diameter air hole is provided on the top surface of the film. When a static load is applied to the hip pad, air in the cell flows out from the air hole and the entire cell gets thinner, leading to a decrease in discomfort during wearing. When an impact load is applied to the hip pad, the resistance of the air enclosed in the cells increases the stiffness of the pad, resulting in the ability to support large impact forces. The sponge in each cell consists of two-layered polyurethanes with different densities. The upper layer is a 5 mm thick high-density sponge (165 kg/m^3) and the lower layer is an 8 mm thick low-density sponge (35 kg/m^3). The high-density sponge has a high impact absorbing performance and the low-density sponge is effective in restoring the shape of each cell quickly

due to the high repulsion performance. The film is made of 0.2-0.25 mm thick polyvinylchloride at the upper layer and sidewall, and the lower layer is 0.3 mm thick.

2.2 Impact testing system

To test the impact absorbing performance of the hip pad, an impact testing system was developed on the assumption of the loading conditions of a fall. Figure 2 is photograph of the impact testing system. After placing hip pads on the load cell (LU-20TE; Kyowa Electronic Instruments, Japan), a weight (Φ97 mm × 170 mm, a mass of 98 N (10 kgf)) is dropped on to the pad. It has been reported that the impact energy of the fall is 100-120 J [(5),(6)]. The potential energy equivalent of this impact energy can be realized by dropping a weight of 98 N (10 kgf) from 1 m. The rating capacity of the load cell is 200 kN, and the data from the load cell was recorded by a sensor interface (PCD-300A; Kyowa Electronic Instruments, Japan). The recording time of the data was set at 1 sec because of the high-speed of the impact test. To record the impact load accurately in the test, an infrared sensor (E3Z-LT; Omuron, Japan) was used to trigger the start of the impact test, and the sensor interface starts recording when the weight passes through the trigger.

2.3 The method of testing

A schematic diagram of impact load measured by load sensor during impact test is shown in Fig. 3. Because it is difficult to specify the time when impact forces are working due to disturbances like noise, the collision time (T=t_1-t_0) is defined as the interval (t_0, t_1) when the impact load is in excess of 5 % of the maximum impact load (P_{max}). The impulse (I) is the integrated value of the impact load during the collision. The mean impact load ($\overline{P}$) is the value obtained by dividing the impulse by the collision time and is calculated by the following Eq. (1).

$$\overline{P} = \frac{I}{T} = \int_{t_0}^{t_1} P(t)\, dt \Big/ (t_1 - t_0) \tag{1}$$

Figure 4 shows the three kinds of hip pads using this impact test: A in Fig.4 is the hip pad with air cushions developed here; B is a commercial soft hip pad (Kotsukotsu hip protector HW3064; Gunze in Japan, 160 mm × 140 mm, 10 mm thick, polystyrene elastomer, 0.78 N (79.6 g)); and C is a commercial hard hip pad (Korobanusakino pants; Dermeister in Japan, 160 mm × 120 mm, 7 mm thick, polyethylene resin, 0.64 N (68.7g))

The relationship between the transmitted impact force and the input energy was examined for the three hip pads with a weight dropped from 10 cm above the surface of the load cell. This height was raised in 10 cm increments up to 1 m. The sampling rate was 5000 Hz and impact

tests were performed three times for each condition. Mean values and standard deviations were calculated.

2.4 Results

The results of the impact tests for the hip pads are shown in Fig. 5-8 (control: no hip pad; A: hip pad with air cushions; B: commercial soft hip pad; and C: commercial hard hip pad). Figure 5 shows the relationship between the maximum impact load (P_{max}) and the input energy (J). The maximum impact load of the control and the hip pads linearly increased as potential energy was higher (correlation coefficient: 0.983 – 0.999). The maximum impact load of the hip pads tended to be lower than that of control. When potential energy was lowest, 9.8 J, values of maximum impact load for each hip pad divided by that for control were respectively 0.27 (hip pad A), 0.37 (hip pad B) and 0.60 (hip pad C). Additionally, When potential energy was highest, 98.1 J, values of maximum impact load for each hip pad divided by that for control were respectively 0.69 (hip pad A), 0.61 (hip pad B) and 0.51 (hip pad C). Figure 6 shows the collision time (T). The collision time of the control and the hip pads linearly decreased as potential energy was higher (correlation coefficient: 0.614 – 0.944). The collision time of the hip pads tended to be longer than that of control. When potential energy was lowest, 9.8 J, values of collision time for each hip pad divided by that for control were respectively 3.84 (hip

pad A), 1.98 (hip pad B) and 1.31 (hip pad C). Additionally, When potential energy was highest, 98.1 J, values of collision time for each hip pad divided by that for control were 2.07 (hip pad A), 1.14 (hip pad B) and 1.43 (hip pad C). Figure 7 shows the mean impact load ($\overline{P}$). The impact load of the control and the hip pads linearly increased as potential energy was higher (correlation coefficient: 0.958 – 0.991). The impact load of the hip pads tended to be lower than that of control. When potential energy was lowest, 9.8 J, values of impact load for each hip pad divided by that for control were respectively 0.23 (hip pad A), 0.34 (hip pad B) and 0.51 (hip pad C). Additionally, When potential energy was highest, 98.1 J, values of impact load for each hip pad divided by that for control were respectively 0.39 (hip pad A), 0.61 (hip pad B) and 0.52 (hip pad C). Figure 8 shows the impulse (I) values. The impulse of the control and the hip pads linearly increased as potential energy was higher (correlation coefficient: 0.963 – 0.980). The impulse was little difference in the control and the hip pads. Most of potential energy for input transferred through each hip pad to the load cell. When potential energy was lowest, 9.8 J, values of impulse for each hip pad divided by that for control were respectively 0.89 (hip pad A), 0.68 (hip pad B) and 0.66 (hip pad C). Additionally, When potential energy was highest, 98.1 J, values of impulse for each hip pad divided by that for control were respectively 0.82 (hip pad A), 0.70 (hip pad B) and 0.75 (hip pad C). Hip pad A was well absorbed impact energy without bouncing the weight under each input potential energy.

3. Experiment to protect against hip fracture

3.1 Specimens

To confirm the effectiveness of the hip pads as protection against hip fracture, impact tests were performed using human femurs. The specimens were cryopreserved four femurs of embalmed cadavers of 3 male and 1 female donors (73-99 years) as shown in Table 1. Before the impact test, femurs were thawed for 10 hours at 20 °C. No obvious fractures were observed in the femurs by X-ray examinations. Robinovitch et al. have reported that soft tissue is effective in force attenuation [(7)], and the skin and subcutis samples were used in the tests here, thicknesses of these samples were 3 mm (skin) and 6 mm (subcutis) respectively.

3.2 The method of the tests

As shown in Fig. 9, the distal part of the femur was bolted to a fixing ring and the femoral head was placed on the load cell with the greater trochanter region upwards. From the results of a finite element analysis for the thigh, Tanaka et al. have reported that the fracture risks are higher in lateral falls than in posterior falls [(8)]. Therefore, the impact tests were performed on the assumption of a lateral fall. The bone axis was set at an angle of 10° from horizontal plane and the femoral neck axis was set at an angle of 90° from horizontal plane, which set was

determined in accordance with most popular impact position in case of lateral falls, as indicated in Fig. 10.

The control had the skin sample on the upper region of the greater trochanter, and two kinds of hip pads with impact force absorption type (hip pad A and B) were placed on the skin sample. For the test of femur No. 3, the subcutis sample was used instead of the skin sample. The weight of 49 N (5 kgf) was used in the impact test, and the dropped height was 20-40 cm from the upper region of greater trochanter. Radiographs were taken after every test. The impact test was performed once for each hip pad at the same dropped height. After testing with the control, the occurrence of fractures was checked by radiographs. If no obvious fractures were observed, the test was performed in the same way with the pads. This procedure was used until a femur was completely fractured. The degree of fracture was determined from the radiographs and observations of impact sites by the orthopedic surgeon (Yukio Nakatsuchi).

3.3 Results

Table 2 shows the degree of the fractures determined from the radiographs (control: no hip pad; A: hip pad with air cushions; B: commercial soft hip pad). The successions of impact tests are in the order from the top of Table 2. "No test" means that this impact test was not performed because the femur was completely fractured in the previous step. The femurs were not

completely fractured by single impact loads but by repeated impact loads lead to spreading of cracks. Three femurs out of four were first cracked in the cancellous bone region of the greater trochanter or the subchondral bone of the femoral head with the control.

The radiographs of femur No. 2 are shown in the order of the tests from the top left in Fig. 11 (I-VI). The white circles in Fig. 11 are the sites of fracture. When the drop height was 20 cm with the control, the cancellous bone region of the greater trochanter cracked (Fig. 11 IV). When the dropped height was 25 cm with hip pad A, there was little difference in the appearance of the crack compared with the previous step (Fig. 11 V). However, with the same drop height with hip pad B, an intertrochanteric fracture occurred and a larger crack was observed from the greater trochanter to the medial cortical bone region (Fig. 11 VI).

4. Discussion

4.1 Impact absorbing performance of hip pads

The three hip pads used in the impact tests reduced the maximum and mean impact loads. The hip pad with air cushions has especially high impact absorption because of a longer collision time and lower mean impact load than the other commercial hip pads. This is because the hip pad with air cushions absorbs the impact force by both the resistance of the air enclosed in cells and of the sponge. A further reason is that the hip pad with air cushions is thicker than

the other hip pads.

The results of past studies with impact tests of hip pads showed that hard hip pads mostly had higher force attenuation effectiveness than soft hip pads [(9), (10)]. These results were obtained in tests using artificial femurs and soft tissue between the hip pad and load cell. The measured impact loads would depend on the geometry and properties of the artificial models. In this study, the impact absorbing performance of hip pads was compared with impact tests of only hip pads. The results showed no obvious differences between soft hip pads (A, B) and the hard hip pad (C). From the results of finite element analysis for the thigh, Tanaka et al. also reported that the materials of hip pads had only little effect in the performance of hip pads [(8)]. If the impact absorbing performance of soft and hard hip pads were little different, as shown above, soft materials would be appropriate for hip pads in terms of comfort during wearing.

4.2 Experiment to protect against hip fracture

The results of the impact tests using human femurs had the first crack occurring with no hip pad in three femurs out of four. The results with hip pad with air cushions showed that the crack spread little after the first crack had been formed. Hence, the hip pad with air cushions would prevent spreading of cracks as well as from causing the first cracks.

Each femur was completely fractured by the repeated impact loads, arising from the spread

of the first crack. The mean value of the maximum impact load in causing the first crack was 1837 N (range 1300-2450 N). This value is similar to the mean femoral fracture load calculated experimentally by Okuizumi et al., 2166 N (range 716-4344 N, SD=944N) [11]. The mean value of the input energy (potential energy of weight) causing the first crack was 14.7 J (range 9.8-19.6 J) in the tests here.

The maximum impact load, collision time, mean impact load and impulse for the impact test using human femurs were calculated. However, the results showed little difference between the condition with and without hip pad. The measured impact load depends on the degree of femoral fracture as well as on the effectiveness of hip pads. Therefore, the impact absorbing performance of hip pads was evaluated from impact tests of only the hip pads without femurs.

Clinical observations show that hip fractures in aged persons by falls are mostly seen in the trochanteric region and the femoral neck. However, in the tests here, the first crack occurred in the femoral head of femurs No. 3 and No. 4. This could be caused by compression forces from the load cell to the femoral head. Especially in the test with femur No. 3, where the subcutis sample was used instead of the skin sample, the femoral head would be subject to a larger applied force than the greater trochanter. Finally, only the femoral head was fractured.

It has been reported that soft tissue is effective in force attenuation. This study also tested the effectiveness of skin samples. A weight of 49 N (5 kgf) was dropped 30 cm from the upper

surface of the load cell. Then, the maximum and mean impact loads were compared for the cases with hip pad A on the 3 mm thick skin sample and in the case with only hip pad A. The maximum and mean impact loads decreased about 20 % and 15 % respectively by addition of the skin sample. Therefore, soft tissue like skin had relatively high force attenuation effectiveness.

4.3 Compliance with hip pads

There are a number of reports of the compliance with hip pad wearing evaluated clinically [(12)-(17)]. Suzuki et al. reported the wearing rates of hard and soft hip pads over six months (20 females aged more than 70) [(14)], showing the wearing rate for soft hip pads as higher (73 %) than that of hard hip pads (44 %). Burl et al. reported the wearing rate for soft hip pads over 13 months (38 females aged 89 on an average) [(15)]. From the results, the mean rate of wearing soft hip pads was above 90 %, and a total of 206 falls were reported, all without hip fractures. These reports indicate that soft hip pads are worn a higher rate than hard hip pads and that they provide sufficient protection against hip fracture.

The reasons for not wearing hip pads are mostly concerned with the difficulty of putting on and taking off the hip pads (especially during toilet), tightness and pressure by underpants and hip pads, and discomfort during wearing [(14), (16)-(18)]. Because the hip pad with air cushions is

lighter than the other hip pads and becomes thinner when deflating under static loads, discomfort during wearing is decreased even in bed. Therefore, a hip pad with air cushions can be expected to improve the rate of wearing hip pads.

5. Conclusions

This report performed impact tests for only hip pads and used human femurs to determine the effectiveness in protection against hip fractures with the hip pad with air cushions. The hip pad with air cushions developed here showed same performance in impact force absorption compared with commercially soft or hard solid type pads under the input energy of range from 9.8 to 98.1J. The Hip pad with air cushions is also sufficiently effective for protection against hip fracture.

Acknowledgment

The authors wish to thank Prof. Tetsuji Moriizumi, MD, Medical School of Shinsyu University, for cooperating with the experiments using human femurs.

References

(1) J. Parkkari, P. Kannus, M. Palvanen, A. Natri, J. Vainio, H. Aho, I. Vuori, M. Jarvinen, Majority of hip fractures occur as a result of a fall and impact on the greater trochanter of the femur: a prospective controlled hip fracture study with 206 consecutive patients. *Calcified Tissue International*, **65**(3) (1999), 183–187.

(2) B.Y. Farahmand, P.G. Persson, K. Michaelsson, J.A. Baron, A. Alberts, T. Moradi, S. Ljunghall, Physical activity and hip fracture: a population-based case-control study. *International journal of epidemiology*, **29**(2) (2000), 308-314.

(3) E.W. Gregg, M. Pereira, C.J. Caspersen, Physical activity, falls, and fractures among older adults: a review of the epidemiologic evidence. *Journal of the American Geriatrics Society*, **48**(8) (2000), 883-893

(4) M.C. Hochberg, D.E. Thompson, D.M. Black, S.A. Quandt, J. Cauley, P. Geusens, P.D. Ross, D. Baran, Effect of alendronate on the age-specific incidence of symptomatic osteoporotic fractures. *Journal of bone and mineral research*, **20**(6) (2005), 971-976.

(5) S. Derler, A.B. Spierings, K.U. Schmitt, Anatomical hip model for the mechanical testing of hip protectors, *Medical Engineering & Physics*, **27**(6) (2005), 475-485.

(6) F. Nabhani, J.S. Bamford, Impact properties of floor coverings and their role during simulated hip fractures, *Journal of Materials Processing Technology*, **153–154** (2004), 139–144.

(7) S.N. Robinovitch, T.A. McMahon, W.C. Hayes, Force attenuation introchanteric soft tissues during impact from a fall, *Journal of Orthopaedic Research*, **13**(6) (1995), 956–962.

(8) E. Tanaka, S. Yamamoto, S. Ozeki, K. Mizuno, A. Harada, M. Mizuno, Biomechanical evaluations of hip fracture prevention by hip protector [in Japanese]. *Transactions of the Japan Society of Mechanical Engineers, Series A,* **70**(697) (2004), 1193-1200.

(9) N.M. Schoor, A.J. Veen, L.A. Schaap, T.H. Smit, P. Lips, Biomechanical comparison of hard and soft hip protectors, and the influence of soft tissue, *Bone*, **39** (2006), 401-407.

(10) P. Kannus, J. Parkkari, J. Poutala, Comparison of Force attenuation properties of four different hip protectors under simulated falling conditions in the elderly: An in vitro biomechanical study, *Bone*, **25**(2) (1999), 229-235.

(11) H. Okuizumi, A. Harada, H. Iwata, N. Konishi, Effect on femur of a new hip fracture preventive system using dropped-weight impact testing, *Journal of Bone and Mineral Research*, **13**(12) (1998), 1940-1945.

(12) A. Harada, M. Mizuno, M. Takemura, H. Tokuda, H. Okuizumi, N. Niino, Hip prevention trial using hip protector in Japanese nursing homes, *Osteoporosis International*, **12** (2001), 215-221.

(13) N.M. Schoor, G. Asma, J.H. Smit, L.M. Bouter, P. Lips, The Amsterdam hip protector study: compliance and determinants of compliance, *Osteoporosis International*, **14** (2003), 353-359.

(14) T. Suzuki, H. Yoshida, T. Ishizaki, H. Yukawa, S. Watanabe, S. Kumagai, S. Shinkai, H. Shibata, T.

Nakamura, S. Yasumura, H. Haga, Compliance in use of external protectors for hip fractures among the community elderly in Japan [in Japanese]. *Nippon Ronen Igakkai Zasshi*, **36** (1999), 40–44.

(15) J.B. Burl, J. Centola, A. Bonner, C. Burque, Hip Protector Compliance: A 13-Month Study on Factors and Cost in a Long-Term Care Facility, *Journal of the American Medical Directors Association*, **4**(5) (2003), 245-250.

(16) N.M. Schoor, W.L. Deville, L.M. Bouter, P. Lips, Acceptance and compliance with external hip protectors: A systematic review of literature, *Osteoporosis International*, **13** (2002), 917-924.

(17) S. Yasumura, T. Suzuki, H. Yoshida, T. Ishizaki, H. Yukawa, S. Watanabe, S. Kumagai, H. Shibata, T. Nakamura, N. Niino, H. Haga, H. Imuta, H. Abe, A. Fukao, Compliance concerning external protectors for hip fractures among the institutionalized elderly in Japan [in Japanese]. *Nippon Ronen Igakkai Zasshi*, **36** (1999), 268–273.

(18) A. Harada, Prevention of hip fractures by hip protectors [in Japanese]. *The Bone*, **17**(3) (2003), 269-272.

Table 1 Particulars of the cadaveric femur specimens

No.	Sex	Age	Body weight (kg)	Length of femur (cm)
1	Male	73	41	45
2	Female	94	34	37
3	Male	99	32	46
4	Male	79	43	44

Table 2 Degree of bone fracture (GT: Greater trochanter, IT: Intertrochanter, FH: Femoral head)

No.	Potential Energy (J)	Dropped height (cm)	Hip pads	Fracture location	Fracture type	Photo Fig. 11	Maximum Impact Load (N)
1	14.7	30	A	No fracture			2000
			B	No fracture			2200
			None	GT cancellous	Crack (15 mm long)		2100
	17.2	35	A	GT cancellous	Crack (20 mm long)		1750
			B	GT cancellous	Crack (40 mm long)		1750
			None	GT cortical and cancellous	Complete fracture		1750
2	9.8	20	B	No fracture		II	1450
			A	No fracture		III	1400
			None	GT cancellous	Crack (20 mm long)	IV	1300
	12.3	25	A	GT cancellous	Crack (20 mm long)	V	1300
			B	IT cortical and cancellous	Complete fracture	VI	950
			None	No test			
3	19.6	40	A	FH subchondral	Crack (25 mm long)		1500
			B	FH subchondral	Complete fracture		1550
			None	No test			
4	14.7	30	A	No fracture			1950
			None	FH subchondral	Crack (13 mm long)		2450
	17.2	35	A	FH subchondral	Crack (13 mm long)		2500
			None	GT cancellous	Crack (20 mm long)		2600

Figure captions

Fig. 1 Hip pad with air cushions

Fig. 2 Impact testing equipment

Fig. 3 Relationship between impact load and time

Fig. 4 Hip pads used in the experiments

Fig. 5 Maximum impact loads

Fig. 6 Collision time

Fig. 7 Mean impact loads

Fig. 8 Impulse (integrated impact load of collision)

Fig. 9 Setting of the specimen for the testing

Fig. 10 Set angles of the femur in the experiments

Fig. 11 Radiographs of femur No.2

Figure 1

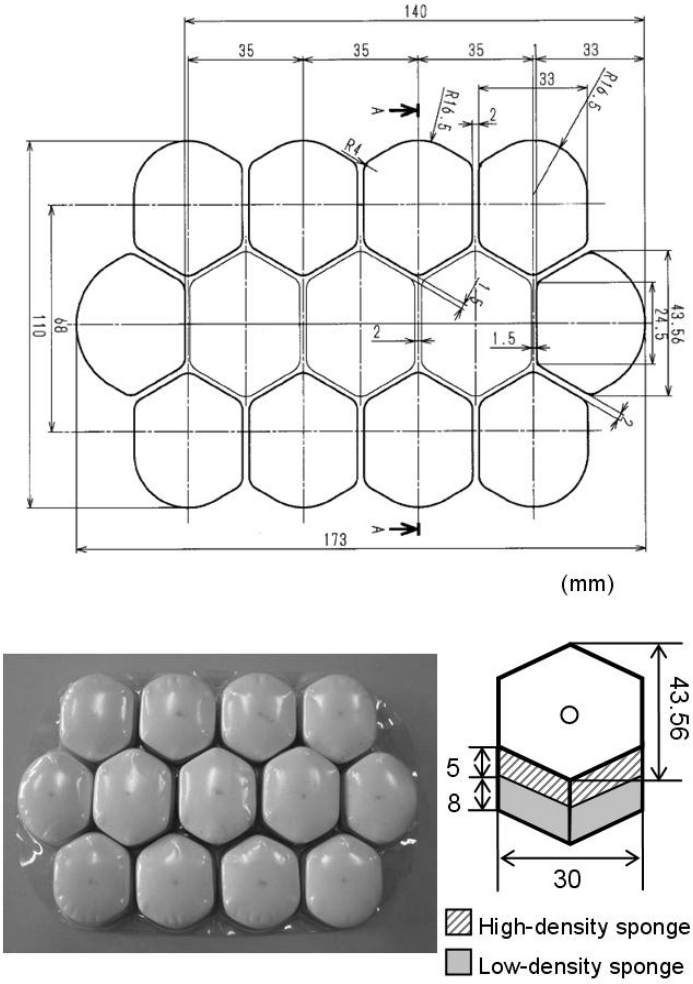
140
35
35
35
33
33
R16.5
R19.5
2
A
R4
110
68
1.5
2
1.5
43.56
24.5
2
173
A
(mm)
43.56
5
8
30
High-density sponge
Low-density sponge

Figure 2

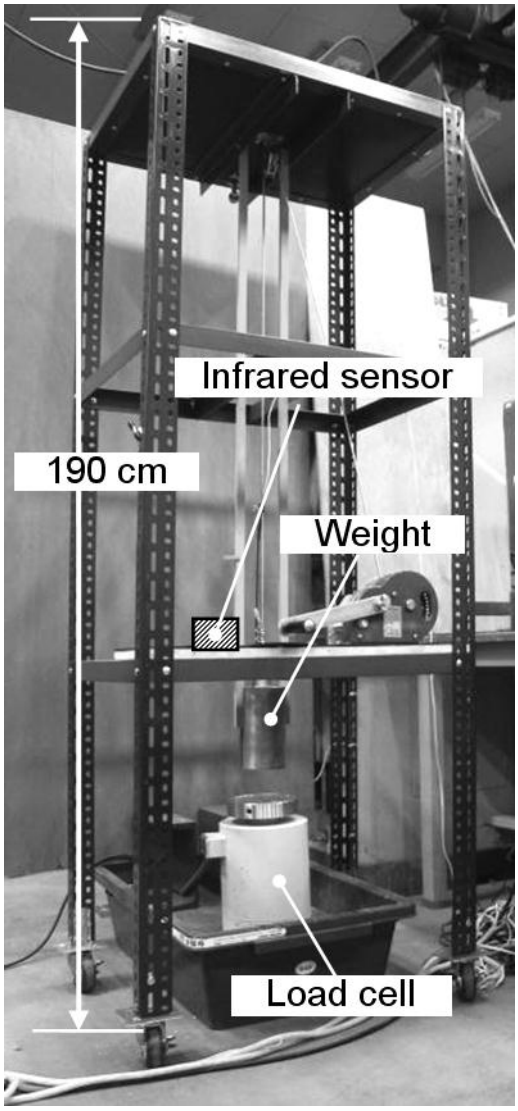

Figure 3

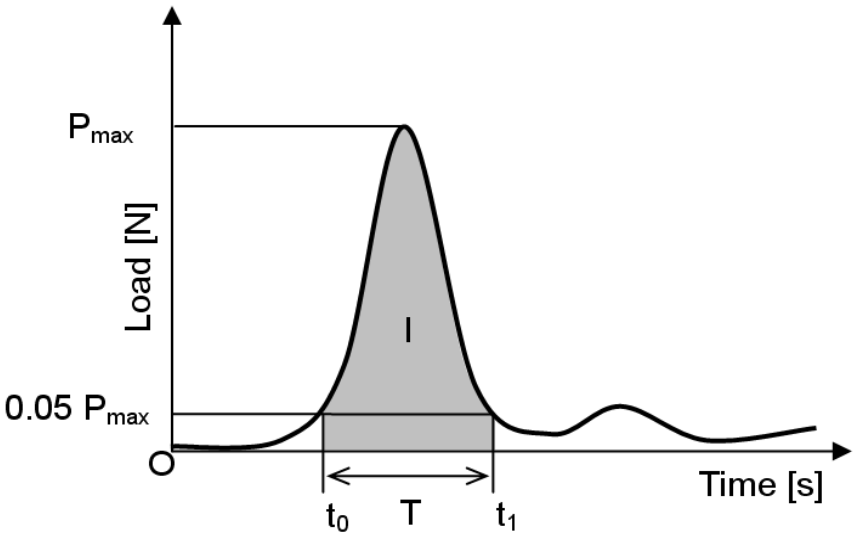

Figure 4

A

B

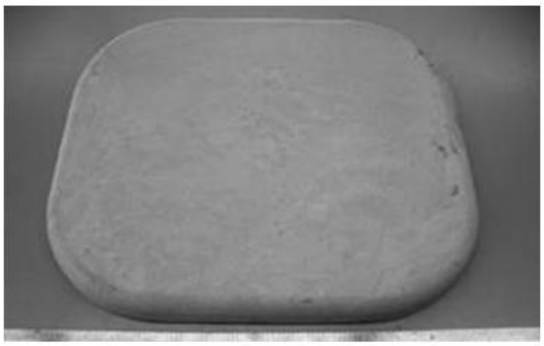

C

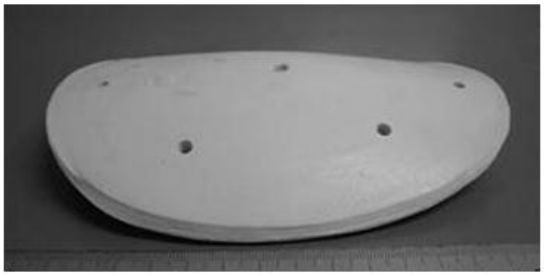

Figure 5

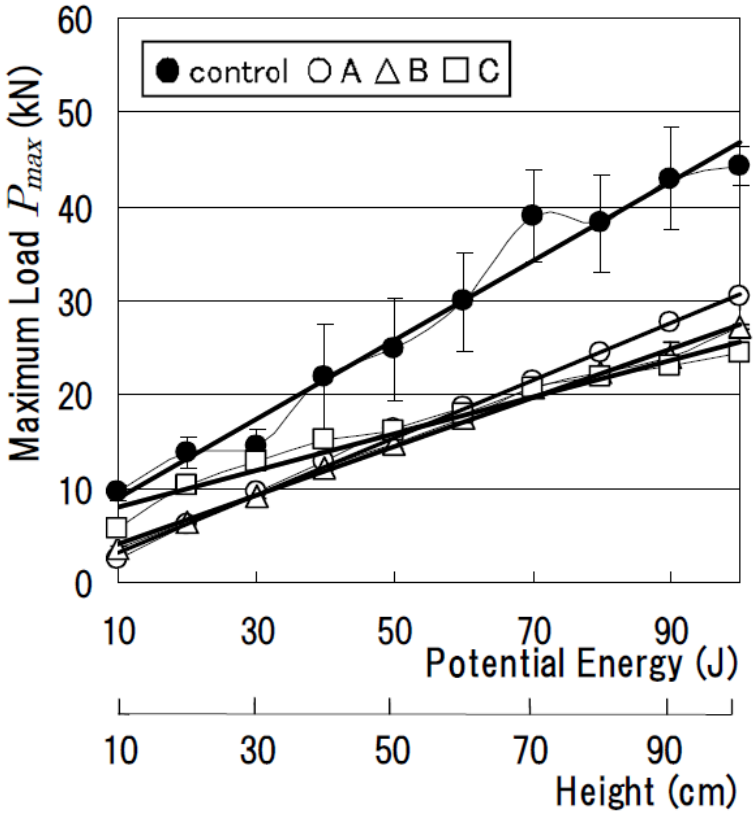
60
50
40
30
20
10
0
Maximum Load P_{max} (kN)
control
A
B
C
10
30
50
70
90
Potential Energy (J)
10
30
50
70
90
Height (cm)

Figure 6

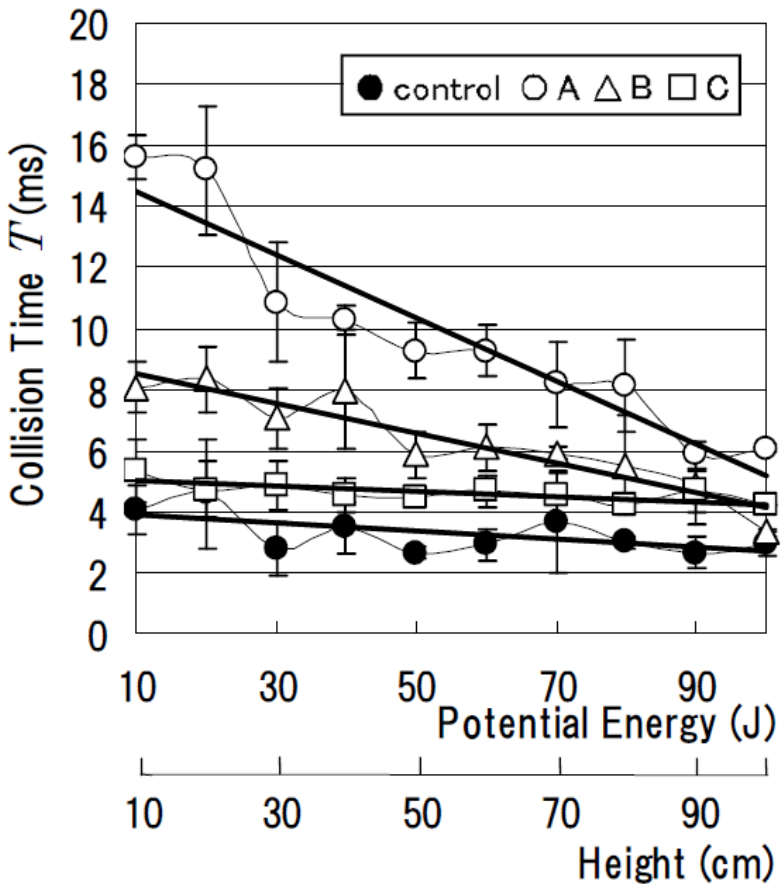
control
A
B
C
Collision Time T (ms)
20
18
16
14
12
10
8
6
4
2
0
10
30
50
70
90
Potential Energy (J)
10
30
50
70
90
Height (cm)

Figure 7

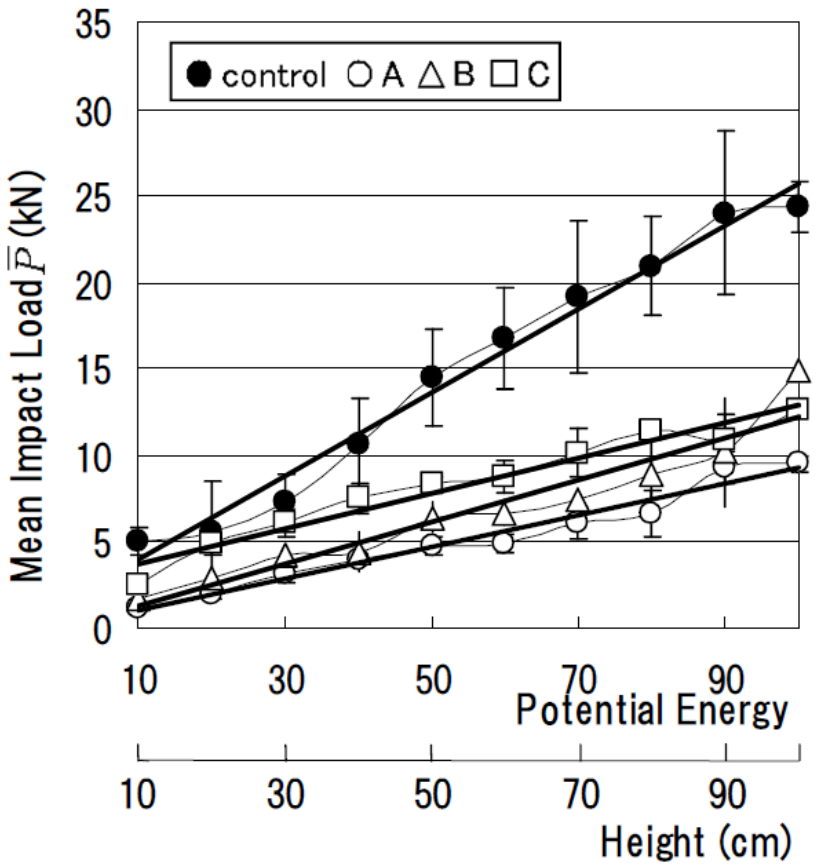
control
A
B
C
Mean Impact Load $\overline{P}$ (kN)
35
30
25
20
15
10
5
0
10
30
50
70
90
Potential Energy
10
30
50
70
90
Height (cm)

Figure 8

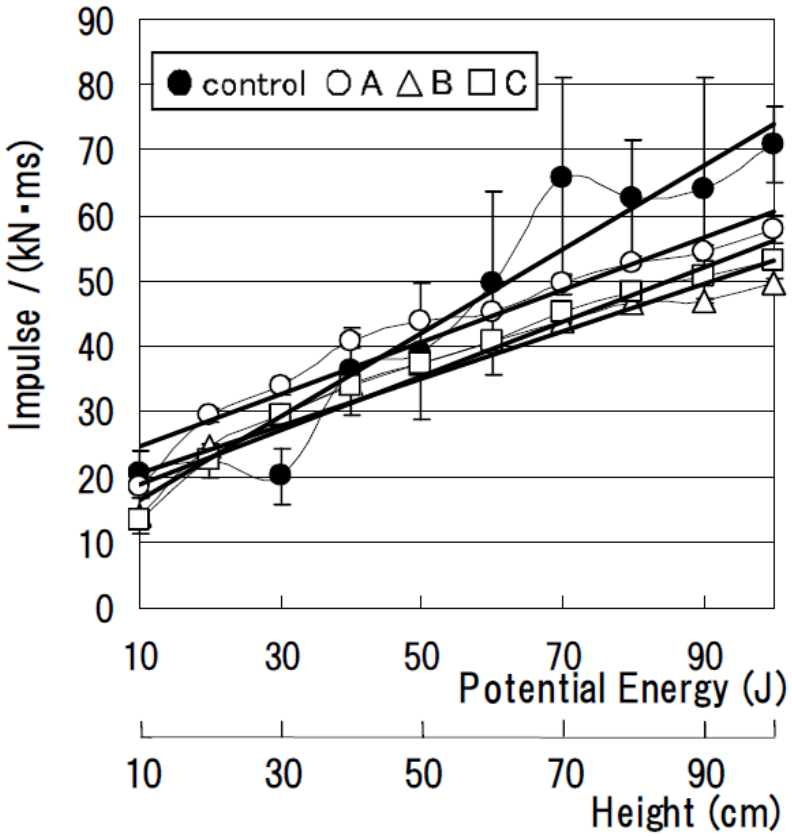
90
80
70
60
50
40
30
20
10
0
Impulse / (kN・ms)
control
A
B
C
10
30
50
70
90
Potential Energy (J)
10
30
50
70
90
Height (cm)

Figure 9

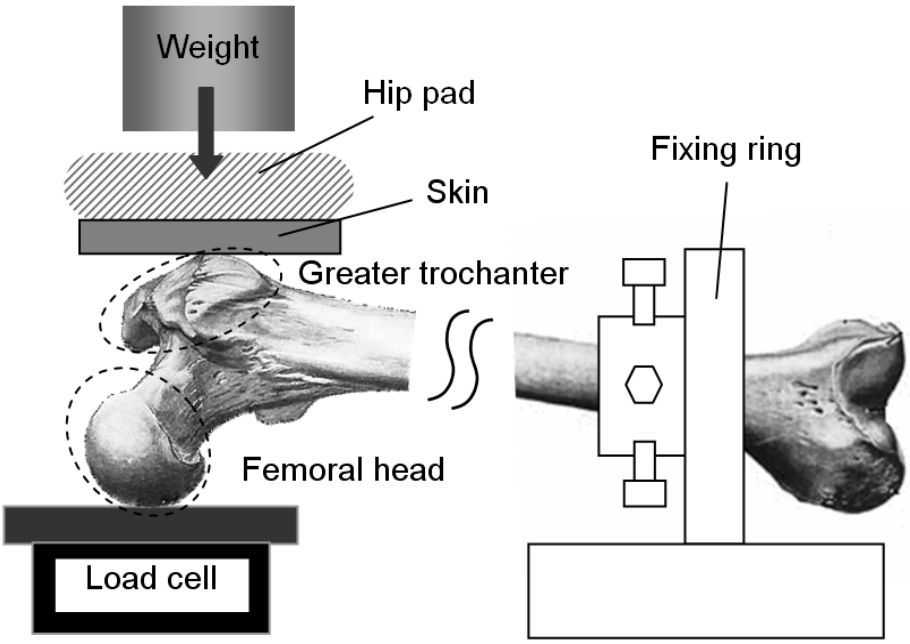
Weight
Hip pad
Skin
Fixing ring
Greater trochanter
Femoral head
Load cell

Figure 10

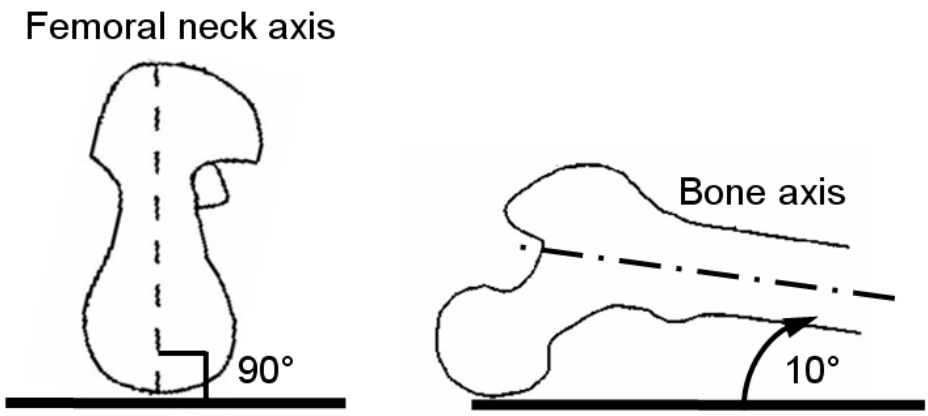

Figure 11

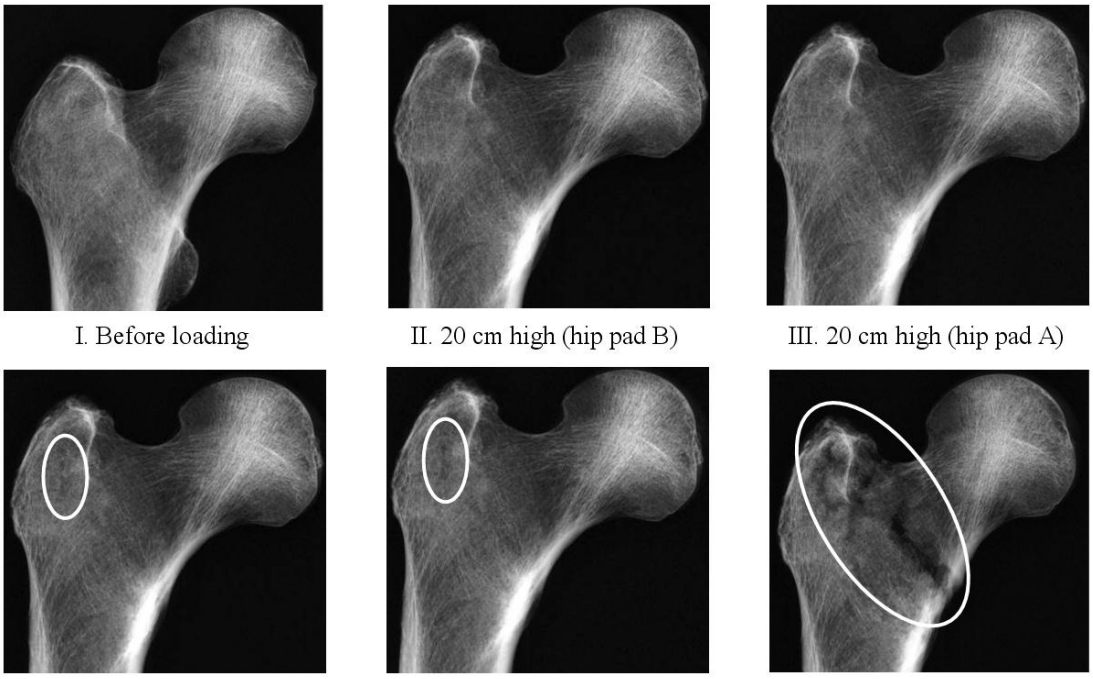

I. Before loading

II. 20 cm high (hip pad B)

III. 20 cm high (hip pad A)

IV. 20 cm high (no hip pad)

V. 25 cm high (hip pad A)

VI. 25 cm high (hip pad B)